JOURNAL *of*
THE KOREAN SOCIETY *of*
RADIOLOGY

Prediction of Amyloid β-Positivity with both MRI Parameters and Cognitive Function Using Machine Learning

뇌 MRI와 인지기능평가를 이용한 아밀로이드 베타 양성 예측 연구

Hye Jin Park, MD[1] (iD), Ji Young Lee, MD[2]* (iD), Jin-Ju Yang, MD[3] (iD),
Hee-Jin Kim, MD[4] (iD), Young Seo Kim, MD[4] (iD),
Ji Young Kim, MD[5] (iD), Yun Young Choi, MD[6] (iD)

Departments of [1]Radiology, [4]Neurology, and [6]Nuclear Medicine, Hanyang University Hospital, Hanyang University College of Medicine, Seoul, Korea
[2]Department of Radiology, Seoul St. Mary's Hospital, College of Medicine, The Catholic University of Korea, Seoul, Korea
[3]Department of Biomedical Engineering, Hanyang University College of Medicine, Seoul, Korea
[5]Department of Nuclear Medicine, Hanyang University Guri Hospital, Hanyang University College of Medicine, Seoul, Korea

ORCID iDs
Hye Jin Park (iD) https://orcid.org/0000-0003-2192-1207
Ji Young Lee (iD) https://orcid.org/0000-0003-1181-8070
Jin-Ju Yang (iD) https://orcid.org/0000-0003-4343-6413
Hee-Jin Kim (iD) https://orcid.org/0000-0001-7880-690X
Young Seo Kim (iD) https://orcid.org/0000-0002-7050-3426
Ji Young Kim (iD) https://orcid.org/0000-0003-2199-4529
Yun Young Choi (iD) https://orcid.org/0000-0002-7535-4343

Purpose To investigate the MRI markers for the prediction of amyloid β (Aβ)-positivity in mild cognitive impairment (MCI) and Alzheimer's disease (AD), and to evaluate the differences in MRI markers between Aβ-positive (Aβ [+]) and -negative groups using the machine learning (ML) method.
Materials and Methods This study included 139 patients with MCI and AD who underwent amyloid PET-CT and brain MRI. Patients were divided into Aβ (+) (*n* = 84) and Aβ-negative (*n* = 55) groups. Visual analysis was performed with the Fazekas scale of white matter hyperintensity (WMH) and cerebral microbleeds (CMB) scores. The WMH volume and regional brain volume were quantitatively measured. The multivariable logistic regression and ML using support vector machine, and logistic regression were used to identify the best MRI predictors of Aβ-positivity.
Results The Fazekas scale of WMH (*p* = 0.02) and CMB scores (*p* = 0.04) were higher in Aβ (+). The vol-

umes of hippocampus, entorhinal cortex, and precuneus were smaller in Aβ (+) ($p < 0.05$). The third ventricle volume was larger in Aβ (+) ($p = 0.002$). The logistic regression of ML showed a good accuracy (81.1%) with mini-mental state examination (MMSE) and regional brain volumes.
Conclusion The application of ML using the MMSE, third ventricle, and hippocampal volume is helpful in predicting Aβ-positivity with a good accuracy.

Index terms Amyloid Beta-Peptides; Third Ventricle; Neuroimaging; Support Vector Machine

INTRODUCTION

Recently, the role of biomarkers such as amyloid β (Aβ) deposition (A), pathologic tau (T), and neurodegeneration (N) in the diagnosis of Alzheimer's disease (AD) has been emphasized by the new 2018 National Institute on Aging and Alzheimer's Association (NIA-AA) Research Framework (1, 2). Among them, amyloid PET, as a test for cerebral Aβ deposition, is widely used as it has high sensitivity and specificity for the discrimination between AD and healthy controls (3). In patients with mild cognitive impairment (MCI), Aβ-positivity is related to the clinical deterioration and rapid progression to dementia (4). Also, higher Aβ levels on PET-CT were correlated with an increased brain atrophy rate in MCI (5). However, amyloid PET has some limitations. In patients with AD, the prevalence of amyloid on PET decreased with age and in patients with most non-AD dementia, that increased with age (6). And amyloid negativity on amyloid PET was observed in 12% of clinically diagnosed AD patients (6). Moreover, amyloid PET also has poor accessibility due to the half-life of pharmaceuticals and its high cost, compared with brain MRI (7, 8).

The role of MRI in diagnosing dementia has focused on the measurement of cerebral atrophy. While atrophy on MR images is not specific for AD, the degree of hippocampal atrophy is sensitive to AD and correlates well with the Braak staging at autopsy (9). Although MRI cannot provide a specific and straightforward diagnosis of AD, MR has a role to rule out structural abnormalities or to identify surgically treatable diseases (9). Recently, many MR studies correlating Aβ pathology and neuroimaging findings have been performed and white matter hyperintensities (WMH) have been studied to investigate their relationship with Aβ-positivity (10). Cerebral amyloid angiopathy and multiple cerebral microbleeds (CMB) have also been associated with AD pathology (11).

Machine learning, as a branch of artificial intelligence, can perform tasks by learning from examples without being programmed (12). Supervised machine learning uses an algorithm for maximizing a particular mathematical function corresponding to a given collection of data (12), thus permitting high-dimensional data analysis (12). Accordingly, machine learning methods have been widely used for the detection and classification of AD, MCI, and prediction of Aβ-positivity in elderly patients (13, 14). Also, machine learning method can be helpful to make the prediction model and to investigate the diagnostic performance of that model.

This study hypothesized that the integration of WMH, CMB, and regional volume could predict Aβ-positivity using multi-MR parameters and machine learning. Our study aimed to investigate MRI markers for the prediction of Aβ-positivity in MCI and AD and to evaluate differ-

ences in WMH, prevalence of CMB, and regional volume between Aβ-positive and -negative groups.

MATERIALS AND METHODS

Our Institutional Review Board approved the study, and the need for informed consent was waived due to the retrospective nature of this study (IRB No. HYUH 2021-07-013).

SUBJECTS

Table 1 shows the demographic and clinical data of the study population. The process of study subject recruitment is shown in Fig. 1. This study used the imaging data of 196 patients who visited the memory clinic at the Hanyang University Hospital and who underwent both MRI and amyloid PET-CT between January 2017 and December 2019. A dementia specialist (neurologist) evaluated scales and neurocognitive function of patients with K-mini-mental state examination (MMSE), clinical dementia rating (CDR), CDR sum of boxes (CDR-SB), global deterioration scale, and caregiver-administered neuropsychiatric inventory (CGA-NPI). The neurologist confirmed the clinical diagnosis of MCI and probable AD, which based on the criteria of the Diagnostic and Statistical Manual of Mental Disorders (4th edition), the National Institute of Neurological and Communicative Disorders and Stroke, and the Alzheimer's Disease and Related Disorders Association (15). The exclusion criteria were as follows: 1) other dementias ($n = 24$), such as Vascular cognitive impairment with no dementia ($n = 10$), Parkinson's dementia ($n = 10$), frontotemporal dementia ($n = 2$), or Lewy-body dementia ($n = 2$), 2) subjective cognitive impairment ($n = 20$), 3) history of other neuropsychiatric symptoms ($n = 10$) including normal pressure hydrocephalus ($n = 6$), mood disorder ($n = 4$), and 4) poor image quality due to MR artifacts ($n = 3$). Finally, 139 patients (60 male, 79 female; age range, 53–95 years; mean age 72.4 years) were included in this study, 92 of whom had MCI and 47 had AD.

ACQUISITION OF AMYLOID PET-CT

All subjects underwent amyloid PET-CT. The amyloid radiotracer, F-18 Florbetaben (Neuraceq, Piramal, Mumbai, India) 8mCi was injected intravenously into the right hand. After a 90-minutes delay, patients were scanned for approximately 20 minutes using a dedicated PET/CT scanner (Biograph 6; Siemens Medical Systems, Knoxville, TN, USA). Aβ-positivity

Table 1. Demographic and Clinical Data of the Study Population

	Amyloid β (+) ($n = 84$)	Amyloid β (-) ($n = 55$)	*p*-Value
Age	73.3 ± 8.7	71.2 ± 8.7	0.20
Sex, male:female	37:47	23:32	0.80
Education	10.0 ± 5.8	10.6 ± 5.4	0.50
MMSE	22.6 ± 5.0	25.8 ± 3.2	< 0.001*
CDR	0.8 (0.5–3.0)	0.6 (0.5–2.0)	< 0.001*
CDR-SB	3.7 (0.5–17.0)	1.0 (0.5–11.0)	< 0.001*

Numbers are presented mean ± standard deviation or median (range).
*Statistically significant.
CDR = clinical dementia rating, CDR-SB = CDR sum of boxes, MMSE = mini-mental state examination

Fig. 1. Study population flow chart.
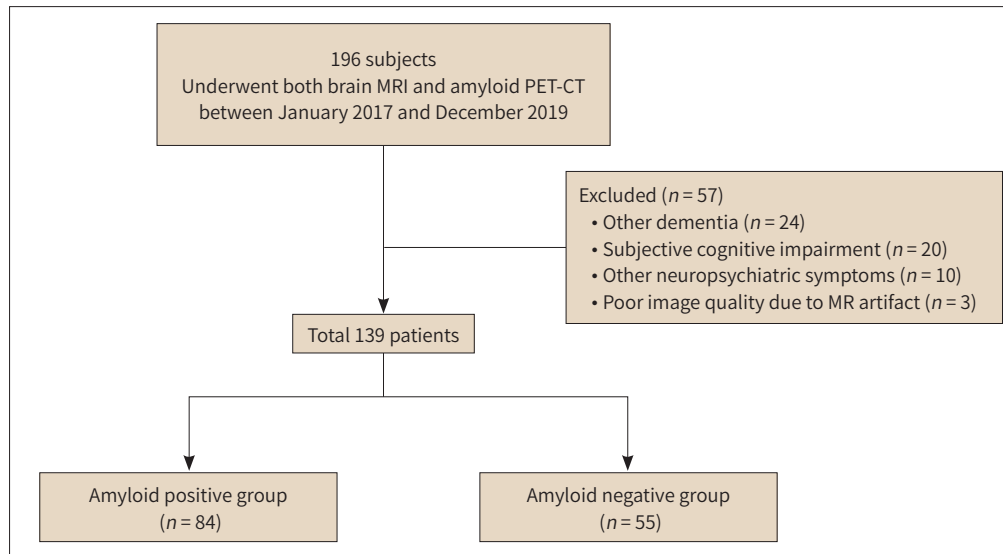
was considered when gray-white matter differentiation was not observed. Two nuclear medicine physicians determined the images to be amyloid-positive or-negative using the visual assessment method. The brain β-amyloid plaque load (BAPL) scoring system was used for group classification (16). Patients with a BAPL score of 1 were classified into the Aβ-negative group, whereas those with scores of 2 or 3 were classified into the Aβ-positive group.

ACQUISITION OF BRAIN MRI

All patients underwent an MRI using a 3T scanner (Ingenia, Philips Healthcare, Best, the Netherlands). The MRI protocol included 3D T1 weighted images, T2 weighted images, fluid attenuated inversion recovery (FLAIR) images, and susceptibility weighted images (SWI) with a coverage of the whole 3D T1WI were acquired. A 3D T1-weighted turbo field echo (TFE) acquisition technique was used for 3D T1WI. The parameters for each sequence were as follows: 3D T1 TFE (repitition time [TR], 8.0 ms; echo time [TE], 3.7 ms; flip angle 8°; field-of-view [FOV], 220 × 220; section thickness 1 mm; matrix 248 × 250; spatial resolution 0.9 mm × 0.9 mm × 1.0 mm), T2WI with turbo spin-echo (TR, 3000 ms; TE, 100 ms; flip angle, 90°; FOV, 220 × 220; section thickness, 5 mm; matrix 420 × 332), FLAIR with fat saturation (TR, 9000 ms; TE, 120 ms; TI, 2500 ms; flip angle, 90°; FOV, 220 × 220; section thickness, 5 mm; matrix 304 × 249), SWI with 3D multi-echo gradient-echo sequence (TR, 31 ms; TE, 17 ms; ΔTE, 6.2 ms; number of echo times, 4; flip angle, 17°; section thickness, 2 mm; matrix, 368 × 368; in-plane resolution, 600 μm). The time interval between the MRI scan and amyloid PET-CT was less than 3 months.

IMAGE ANALYSIS OF WMH, CMB AND REGIONAL VOLUME

All images were interpreted by a neuroradiologist (J.Y.L.) and a trainee radiologist (H.J.P.), both of whom were blinded to the subjects' clinical information. The radiologists evaluated the WMH on FLAIR images. The degree of WMH was scored using the Fazekas scale, which shows the sum of periventricular and deep WMH (10, 17). The presence, number, and location

of CMBs were reviewed on SWI images. We confirmed the low signal intensity foci of CMBs on the corresponding phase maps in the right-handed MR coordinate system. Additionally, we investigated the presence of lacunar infarct, cortical infarct, and superficial siderosis (18-20). For the quantitative analysis, we used the automated segmentation software DeepBrain® (VUNO Med®, Seoul, Korea) from 1-mm slice thickness 3D T1 TFE images (21). We obtained 57 regional brain volumes. The WMH volume was obtained using automated brain segmentation software (UBO Detector, https://cheba.unsw.edu.au/group/neuroimaging-pipeline) from 5-mm slice thickness FLAIR images (22).

STATISTICAL ANALYSIS

For the comparisons between Aβ-positive and Aβ-negative groups, continuous variables were expressed as means and standard deviations. The Kolmogorov–Smirnov test was performed to determine whether the values were normally distributed. An independent *t* test was used to compare each imaging parameter between the two groups. Fisher's exact test was used to compare categorical variables. Qualitative and quantitative results were compared between the two groups. Multivariable logistic regression analysis was performed to investigate the MR factors related to Aβ-positivity. And subgroup analysis was performed in patients with only MCI. The group comparisons and multivariable logistic regression analysis was also performed in patients with MCI. Statistical analyses were performed using commercially available software (SPSS, version 24 for Windows; IBM Corp., Armonk, NY, USA).

MACHINE LEARNING CLASSIFICATION

We adopted a support vector machine (SVM) and logistic regression, which are frequently used in many classification studies, and evaluated binary classification performance between the Aβ-positive and the Aβ-negative groups using Python's scikit learning library (https://github.com/scikit-learn/scikit-learn) (23, 24). Statistically significant volume features were initially obtained from the previous step of univariate logistic regression, including the left and right hippocampus, entorhinal cortex, precuneus, parietal lobe, third ventricle, and inferior lateral ventricle volume. MMSE was additionally included as an input variable since it was most significantly correlated with Aβ-positivity. Feature selection was then performed using the recursive feature elimination (RFE) method on five-fold cross-validation with a random forest classifier as an estimator to find optimal features for machine learning model training (25, 26). Finally, nine features were selected as inputs for SVM and logistic regression classifiers including MMSE scores, the volume of left and right hippocampus, left entorhinal cortex, left precuneus cortex, parietal lobe, third ventricle, and left inferior lateral ventricle. All observations were randomly divided into five equal-size partitions and trained on four partitions, while the classification performance was tested on the holdout partition. Classification performance was calculated by comparing the accuracy, sensitivity, specificity, positive predictive value (PPV), negative predictive value (NPV), and the area under the receiver operating characteristic (ROC) curve (AUC). The model parameters were optimized for each classifier based on five-fold cross-validation. This procedure was repeated five times to avoid the overfitting of the test set and to improve the generalization.

RESULTS

The participants were divided into an Aβ-positive (*n* = 84) and an Aβ-negative (*n* = 55) group. Aβ-positivity was observed in 60.4% of patients. In the Aβ-positive group, 45 patients had MCI (53.6%) and 39 had AD (46.4%). In the Aβ-negative group, 47 patients had MCI (85.5%) and

Fig. 2. Representative case of amyloid β-positive group. A representative case of an 81-year-old male with Alzheimer's disease.
A. According to the RCTB scoring system, all eight brain regions were graded with pronounced binding (score 3). Therefore, Amyloid PET-CT finding is considered a significant β-amyloid load and has a BAPL score of 3.
B. The fluid attenuated inversion recovery image shows periventricular white matter hyperintensities.
C. On susceptibility weighted image, multiple microbleeds are shown in the lobar location.
D. On 3D T1 turbo field echo image axial scan, the third ventricle shows dilatation.
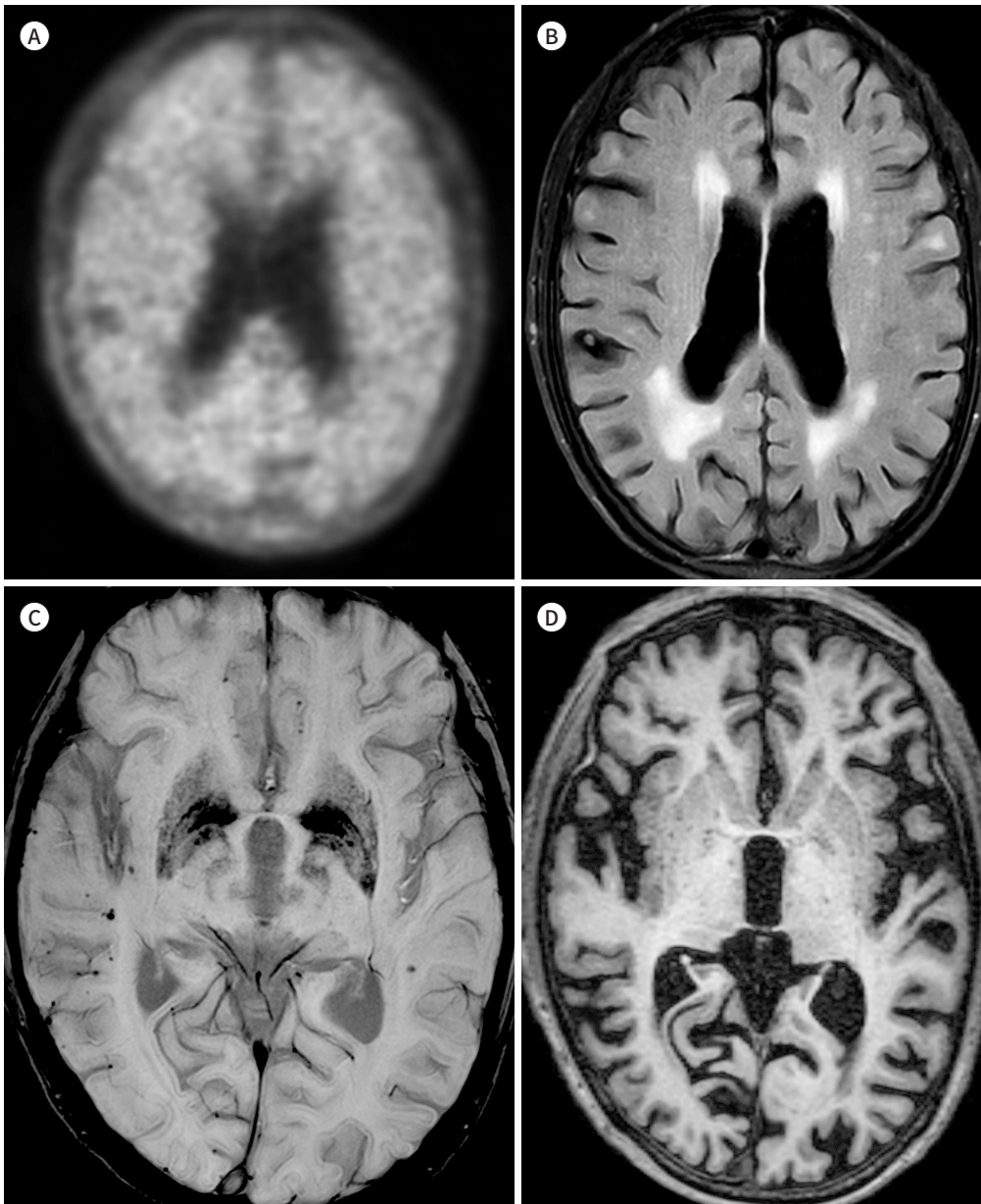
eight had AD (14.5%). Among the patients with MCI, the Aβ-positivity and Aβ-negativity rates were 48.9% and 51.1%, respectively. Among the patients with AD, Aβ-positivity and Aβ-negativity rates were 83% and 17%, respectively. There was no significant difference in age or sex between the two groups (Table 1). Regarding clinical assessment, there was a significant dif-

Fig. 3. Representative case of amyloid β-negative group. A representative case of a 68-year-old male with MCI.
A. According to the RCTB scoring system, all eight brain regions were graded with no binding (score 1). Therefore, amyloid PET-CT finding is considered as having no amyloid-β load (BAPL score of 1) and a negative PET-scan.
B. On fluid attenuated inversion recovery images, there is no hyperintensity in the periventricular or deep white matter.
C. On susceptibility weighted image, there is no cerebral microbleed.
D. On the 3D T1 turbo field echo image axial scan, the third ventricle was not dilated.
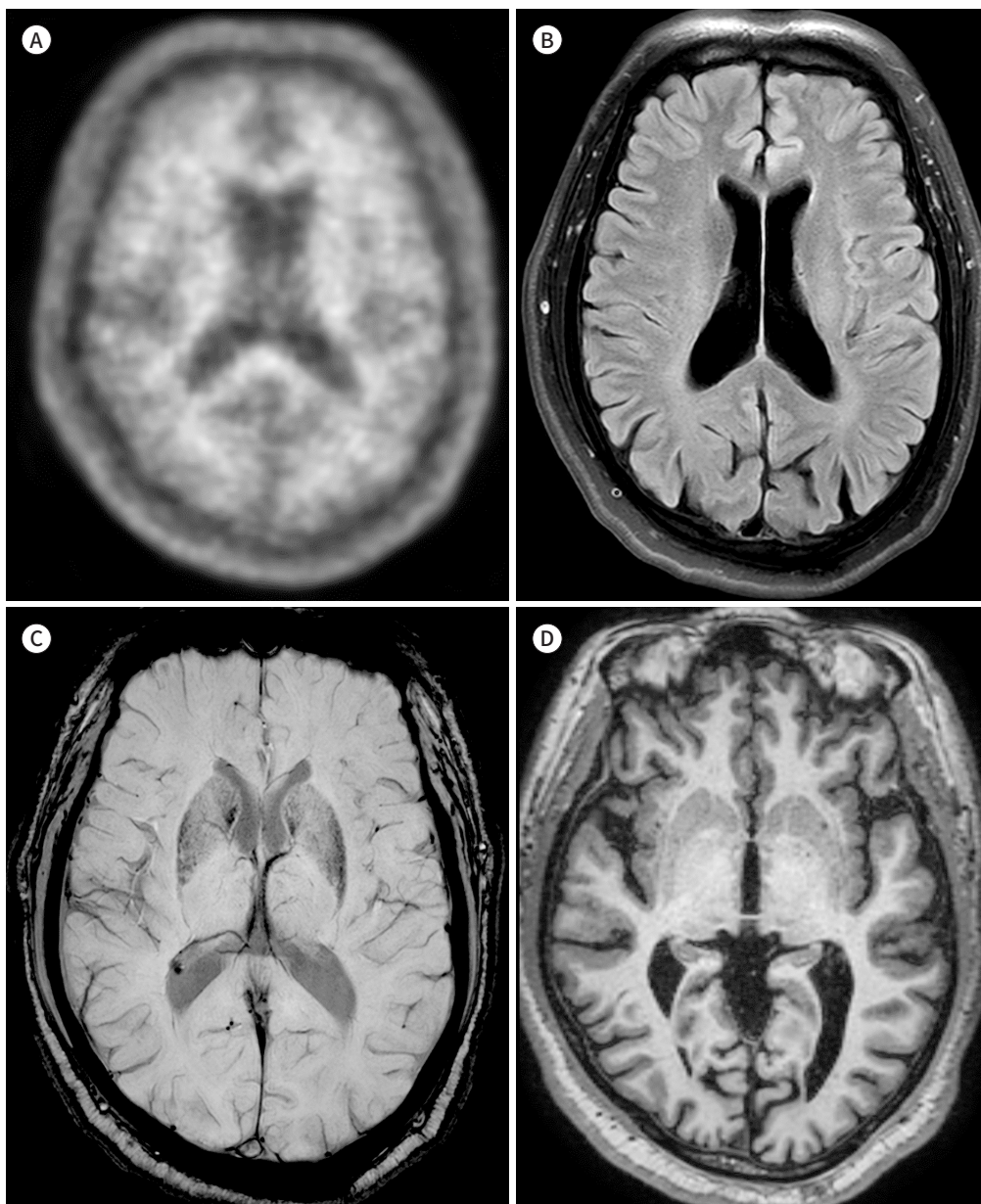
ference between the groups in terms of MMSE, CDR, and CDR-SB scores.

For the qualitative analysis, the Aβ-positive group showed significantly higher Fazekas scale of WMH and CMB scores ($p = 0.02$ and $p = 0.038$, respectively) (Figs. 2, 3). There were no significant differences in lacunar infarct, cortical infarct, and superficial siderosis between the two groups (Table 2).

For the quantitative analysis, although there was no significant difference in WMH volume, the Aβ-positive group showed a larger volume of WMH (Table 3). For the regional volume analysis, there were significant differences in both hippocampus, entorhinal cortex, left parahippocampus, left fusiform gyrus, left parietal lobe, right occipital lobe, and both precuneus between the two groups ($p < 0.05$) (Table 3). The third ventricle and inferior lateral ventricle were significantly larger in the Aβ-positive group than in the Aβ-negative group ($p = 0.002$ in the third ventricle, $p = 0.003$ in the left inferior lateral ventricle, and $p = 0.001$ in the right inferior lateral ventricle, Figs. 2, 3).

Multivariable logistic regression was performed to find the best MR imaging factor related to amyloid positivity. Univariable logistic regression analysis was performed, and multivariable logistic regression was performed using the significant MRI markers. The MMSE and third ventricle volume were the most significant factors for predicting Aβ-positivity (Table 4).

This study performed the subgroup analysis in patients with only MCI (Supplementary Tables 1-3 in the online-only Data Supplement). There was no significant difference of MMSE between two groups in patients with MCI. The Aβ-positive MCI group showed significantly higher CMB numbering and less frequent lacunar infarct than Aβ-negative MCI group ($p = 0.04$, and $p < 0.001$, respectively). For the regional volumes, Aβ-positive MCI group demonstrated significantly smaller volume of entorhinal cortex, and significantly larger volume of right inferior lateral ventricle and fourth ventricle volume ($p = 0.02$, and $p < 0.001$ in left and right entorhinal cortex, 0.01 in the right inferior lateral ventricle and 0.007 in fourth ventricle). The multivariable logistic regression showed the lacunar infarct is the most significant factor with Aβ- positivity ($p = 0.047$, odds ratio = 0.36).

Table 2. The Comparison of Qualitative Analysis between Two Groups

	Amyloid β (+) ($n = 84$)	Amyloid β (-) ($n = 55$)	*p*-Value
Fazekas scale, WMH	3.0 ± 1.4	2.4 ± 1.3	0.02*
CMB numbering	3.9	1.0	0.04*
Lacunar infarct			0.20
Yes	18	16	
No	66	35	
Cortical infarct			0.50
Yes	3	3	
No	81	48	
Superficial siderosis			0.07
Yes	0	2	
No	84	49	

*Statistically significant.
CMB = cerebral microbleed, WMH = white matter hyperintensities

Table 3. The Results of Quantitative Regional Brain Volume Analysis between Two Groups

	Amyloid β (+) (*n* = 84)	Amyloid β (-) (*n* = 55)	*p*-Value
WMH, cc			
Volume, WMH	17250.0 ± 14697.4	13442.89 ± 12449.26	0.13
Volume, periventricular WMH	12428.12 ± 9734.72	9791.47 ± 8559.16	0.11
Volume, deep WMH	4653.52 ± 5829.83	3489.69 ± 4203.78	0.22
Brain regional volume			
Hippocampus, Lt	3.15 ± 0.59	3.57 ± 0.60	< 0.001*
Hippocampus, Rt	3.53 ± 0.67	4.30 ± 0.68	< 0.001*
Amygdala, Lt	1.11 ± 0.24	1.11 ± 0.24	0.97
Amygdala, Rt	1.35 ± 0.26	1.44 ± 0.27	0.06
Entorhinal cortex, Lt	1.69 ± 0.65	2.52 ± 0.47	< 0.001*
Entorhinal cortex, Rt	1.88 ±1.15	3.18 ± 0.43	< 0.001*
Parahippocampus, Lt	1.51 ± 0.34	1.63 ± 0.32	0.03*
Parahippocampus, Rt	1.34 ± 0.27	1.39 ± 0.21	0.24
Fusiform gyrus, Lt	7.22 ± 1.42	7.790 ± 1.08	0.01*
Fusiform gyrus, Rt	6.82 ± 1.29	7.21 ± 1.02	0.06
Temporal lobe, Lt	43.87 ± 6.41	44.26 ± 5.17	0.71
Temporal lobe, Rt	42.20 ± 5.96	41.25 ± 5.07	0.34
Frontal lobe, Lt	60.76 ± 7.19	62.19 ± 5.83	0.22
Frontal lobe, Rt	61.0 ± 6.84	61.92 ± 5.87	0.41
Parietal lobe, Lt	41.11 ± 5.98	43.19 ± 4.63	0.03*
Pariteal lobe, Rt	41.60 ± 4.80	43.85 ± 4.49	0.01*
Occipital lobe, Lt	16.87 ± 2.6	17.58 ± 2.05	0.09
Occipital lobe, Rt	16.98 ± 2.48	17.77 ± 1.95	0.04*
Gray matter cortex, Lt	176.73 ± 21.14	183.89 ± 17.94	0.04*
Gray matter cortex, Rt	170.65 ± 19.37	168.25 ± 17.10	0.45
Third Ventricle	2.12 ± 0.73	1.78 ± 0.65	0.01*
Fourth Ventricle	2.19 ± 0.63	2.22 ± 0.40	0.77
Lateral ventricle, Lt	21.87 ± 8.95	20.05 ± 9.25	0.25
Lateral ventricle, Rt	20.88 ± 8.84	18.01 ± 8.73	0.06
Inferior lateral ventricle, Lt	1.54 ± 0.9	1.15 ± 0.6	0.01*
Inferior lateral ventricle, Rt	1.43 ± 0.92	1.00 ± 0.59	0.01*
Precuneus cortex, Lt	7.08 ± 1.04	7.62 ± 1.15	0.01*
Precuneus cortex, Rt	7.43 ± 0.93	7.95 ± 1.21	0.01*

*Statistically significant.
WMH = white matter hyperintensities

CLASSIFICATION PERFORMANCE OF MACHINE LEARNING METHODS

We compared the performance results of the two classifiers with the RFE feature selection in Table 5. With an accuracy of 81.1%, the logistic regression classifier had a higher performance than the SVM, which had an accuracy of 78.4%. The sensitivity, specificity, PPV, NPV, and AUC for the logistic regression classifier were 91.6%, 65.5%, 80.4%, 85.3%, and 79.0% respectively. The ROC curve is shown in Fig. 4. In contrast, the SVM classifier had a sensitivity, specificity, PPV, NPV, and AUC of 78.2%, 78.6%, 84.6%, 72.1%, and 78%, respectively.

Table 4. Logistic Regression Analysis to Identify the Variables for Predicting Amyloid Positivity

	Odds Ratio	*p*-Value
Mini-mental state examination	0.87	0.017*
Third ventricle volume	1.98	0.034*

*Statistically significant.

Table 5. Machine Learning Methods Results with Comparison of the Classification Performance

Classifier	AUC	ACC (%)	Sensitivity (%)	Specificity (%)	PPV (%)	NPV (%)
RFE feature selection (*n* = 9)						
SVM	0.78	78.4	78.2	78.6	84.6	72.1
LR	0.79	81.1	91.6	65.5	80.4	85.3
Univariate feature selection (*n* = 13)						
SVM	0.74	75.2	81.3	66.8	77.7	72.4
LR	0.76	78.4	88.8	63.3	78.0	80.8

ACC = accuracy, AUC = area under the curve, LR = logistic regression, NPV = negative predictive value, PPV = positive predictive value, RFE = recursive feature elimination, SVM = support vector machine

With regard to the performance of the feature selection approach in the logistic regression classifier (Table 5), the RFE feature selection results revealed higher performances in all values than those of the univariate feature selection (the accuracy; 81.1% in RFE vs. 78.4% in univariate selection). The SVM classifier also showed slightly higher performance with the RFE feature selection (accuracy; 78.4% in RFE vs. 75.2% in univariate selection) than it did with the univariate feature selection, with the exception of specificity.

DISCUSSION

This study found the best predictor Aβ-positivity to be the MMSE score and regional volume, including the third ventricle, hippocampus, entorhinal cortex, and precuneus in the multivariable logistic regression. The machine learning method had a good accuracy of 81.1%, for predicting Aβ-positivity using the MMSE score and regional brain volumes. This study results showed the differences between the Aβ-positive and -negative groups using multi-MRI parameters, WMH, CMB, and regional volumes. The Aβ-positive group showed lower MMSE scores, higher CDR and CDR-SB scores, and high WMH and CMB scores. The regional volumes of the hippocampus, entorhinal cortex, parietal lobe, and precuneus were lower in the Aβ-positive group. The third ventricle and inferior lateral ventricle were significantly larger in the Aβ-positive group. In subgroup analysis, the Aβ-positive MCI group showed higher CMB numbering and less frequent lacunar infarction than the Aβ-negative MCI group.

Previous studies have found that various imaging markers are associated with Aβ-positivity. A study compared the regional volumes between Aβ-positive and negative groups in patients with MCI and showed that the normative percentiles of hippocampal volume were the best predictors, with an AUC of 0.723 (27). Another study showed that Aβ-positive subjects had significantly higher WMH volumes than Aβ-negative subjects in patients with AD and healthy

Fig. 4. Machine learning ROCs curves.
A-D. Curves from logistic regression machine learning (A, B) and support vector machine (C, D) with recursive feature elimination feature selection (A, C), and univariate feature selection (B, D) are demonstrated.
AUC = area under the curve, ROC = receiver operating characteristic, SD = standard deviation
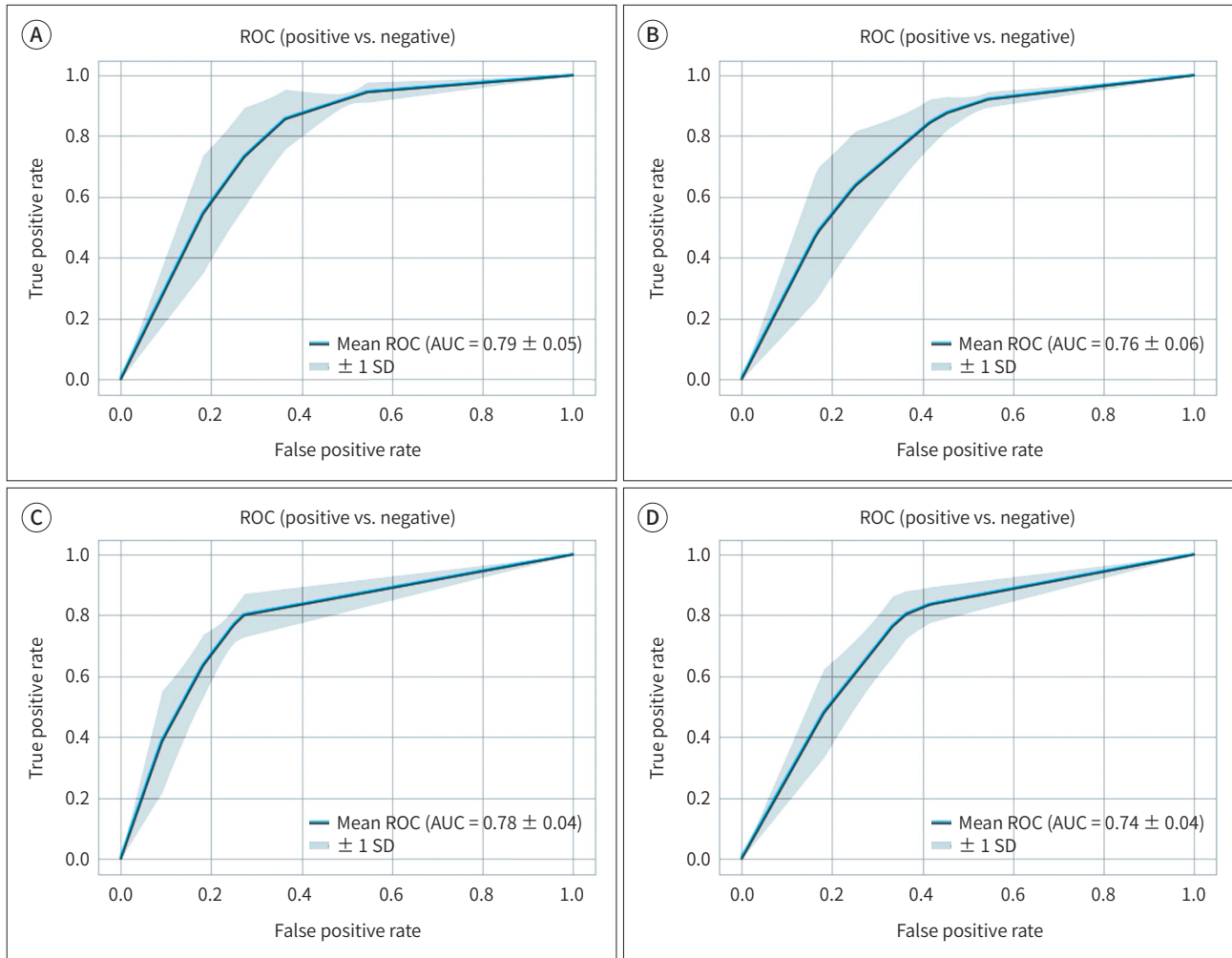
controls (10). A study demonstrated that CMB is related to the global and frontal Aβ load (11). Our study results are consistent with those of previous studies on regional volume, WMH, and CMB scores. The difference is that this study investigated multi-MRI parameters, and among them, the third ventricle volume was the most significant predictor of Aβ-positivity.

This study used the machine learning technique, SVM, and logistic regression to evaluate the Aβ predictability of MRI markers. A previous group reported that machine learning models can predict Aβ-positivity using clinical feature models and brain MRI feature models in patients with amyloid angiopathy or MCI (13, 14). They showed an AUC of 0.80–0.83 with MRI features using a tree-based machine learning method to predict amyloid positivity in patients with amyloid angiopathy (13). Another study using radiomics showed an AUC of 0.79 to predict amyloid positivity in patients with MCI (28). Our study showed a similar good performance of logistic regression machine learning with the RFE feature selection method, demonstrating an AUC of 0.79 with 81% accuracy. Because Aβ-positivity is important to diagnose AD as well as to pre-

dict the prognosis of patients, Aβ-positivity prediction using MMSE and several regional volumes could be very useful in clinical practice (28, 29).

The results of this study showed that the volume change of the third ventricle could be the most significant MR factor in predicting Aβ-positivity. A study reported that ventricle enlargement could be observed in patients with AD due to altered CSF dynamics, and ventricle enlargement can be associated with decreased levels of Aβ (30). Accordingly, decreased amyloid in CSF could be attributable to the amyloid deposits in the brain, which could be visually detectable on amyloid PET-CT. In our experiences, third ventricle enlargement is easy to detect and useful to compare with other patients, although it can be subjective, and we did not provide the cutoff values of the third ventricle volume to discriminate Aβ-positive from Aβ-negative groups. Therefore, we assume that the assessment of third ventricle enlargement could be a helpful imaging marker to predict Aβ in clinical practice.

The Aβ-positive group showed a tendency towards a larger WMH volume, although the difference was not statistically significant. Additionally, more CMBs were observed in the Aβ-positive group. The pathophysiology of Aβ-related WMH could be explained by several hypotheses: oligodendrocyte dysfunction and demyelination with axonal degeneration, cerebrovascular pathology, endothelial dysfunction, or BBB dysfunction (31). CMB could be a factor associated with vessel integrity and is also known as an imaging marker of amyloid angiopathy (28). Thus, we hypothesized that CMB could be an important factor in predicting Aβ-positivity. CMBs were frequently observed in this study; however, it was not a critical factor in predicting Aβ-positivity. A previous study showed that CMB could be related to ventricular enlargement in patients with MCI (32). It is possible that the different results maybe be due to different study populations and study designs. Thus, further studies are needed to demonstrate the relationship between WMH, CMB, and ventricular dilatation in patients with MCI or AD.

In subgroup analysis with only MCI patients, Aβ-negative group showed significantly more frequent lacunar infarct than Aβ-positive group. In the multivariable logistic regression, lacunar infarction is the only significant factor with an odds ratio 0.36. This can be difficult to explain, because it is not well studied about the association between the amyloid pathology and lacunar infarct. However, this result could be supported by a study which shows that silent lacunar infarct, as a component of small vessel disease, is associated with cognitive decline (33). Also recent memory impairment was the most often impaired cognitive domain after lacunar infarct (34). In MCI patients without amyloid positivity, the lacunar infarct was probable main cause of cognitive impairment in this study group.

This study had several limitations. First, this was a retrospective study with a selection bias. Second, we conducted correlation studies between amyloid PET-CT imaging and MRI only, but excluded tau imaging. The pathology of AD includes tau pathology as well as amyloid deposition; therefore, the MRI factor associated with tau could also be important. Further studies investigating the MRI factors related to tau are needed in the future. We performed a cross-sectional study; and therefore, we did not consider the longitudinal atrophy rate, which might be a more specific indicator of Aβ-positivity. Third, the subgroup analysis was performed for only MCI patients, but the results did not show the same results to those obtained from patients with MCI and AD. For MCI patients, the lacunar infarct was a significant factor to predict the Aβ-positivity. The MMSE and third ventricle volume cannot be applied to predict the

amyloid positivity in the patients with MCI. Finally, the performance of machine learning in predicting amyloid positivity was not better than previous studies. Thus, it is possible that the unknown key for predicting amyloid positivity might be related to clinical or serologic factors rather than imaging features. Further, we did not consider the status of the apolipoprotein E ε4 genotype, which might have enhanced the performance of the machine learning method.

In conclusion, the Aβ-positive group showed lower MMSE scores, higher volumes of WMH, more frequent CMBs, and regional brain volume changes. The machine learning method exhibited good accuracy in predicting Aβ-positivity with the MMSE score and regional volume, including the third ventricle, hippocampus, entorhinal cortex, and precuneus.

Supplementary Materials

The online-only Data Supplement is available with this article at http://doi.org/10.3348/jksr.2022.0084.

Author Contributions

Conceptualization, L.J.Y.; data curation, P.H.J., K.H.; formal analysis, P.H.J., L.J.Y., Y.J.; investigation, P.H.J., L.J.Y., Y.J.; methodology, L.J.Y.; project administration, L.J.Y.; resources, K.H., C.Y.Y.; software, Y.J.; validation, P.H.J., L.J.Y.; visualization, P.H.J., L.J.Y., Y.J.; writing—original draft, P.H.J., L.J.Y.; and writing—review & editing, P.H.J., L.J.Y., K.Y.S., K.J.Y.

Conflicts of Interest

The authors have no potential conflicts of interest to disclose.

REFERENCES

1. Jack CR Jr, Bennett DA, Blennow K, Carrillo MC, Feldman HH, Frisoni GB, et al. A/T/N: an unbiased descriptive classification scheme for Alzheimer disease biomarkers. *Neurology* 2016;87:539-547
2. Jack CR Jr, Bennett DA, Blennow K, Carrillo MC, Dunn B, Haeberlein SB, et al. NIA-AA research framework: toward a biological definition of Alzheimer's disease. *Alzheimers Dement* 2018;14:535-562
3. Marcus C, Mena E, Subramaniam RM. Brain PET in the diagnosis of Alzheimer's disease. *Clin Nucl Med* 2014;39:e413-e422
4. Okello A, Koivunen J, Edison P, Archer HA, Turkheimer FE, Någren K, et al. Conversion of amyloid positive and negative MCI to AD over 3 years: an 11C-PIB PET study. *Neurology* 2009;73:754-760
5. Tosun D, Schuff N, Mathis CA, Jagust W, Weiner MW; Alzheimer's Disease NeuroImaging Initiative. Spatial patterns of brain amyloid-beta burden and atrophy rate associations in mild cognitive impairment. *Brain* 2011;134(Pt 4):1077-1088
6. Ossenkoppele R, Jansen WJ, Rabinovici GD, Knol DL, van der Flier WM, van Berckel BN, et al. Prevalence of amyloid PET positivity in dementia syndromes: a meta-analysis. *JAMA* 2015;313:1939-1950
7. Wolk DA, Price JC, Saxton JA, Snitz BE, James JA, Lopez OL, et al. Amyloid imaging in mild cognitive impairment subtypes. *Ann Neurol* 2009;65:557-568
8. Landau SM, Horng A, Fero A, Jagust WJ; Alzheimer's and MCI. *Neurology* 2016;86:1377-1385
9. Jack CR Jr. Alzheimer disease: new concepts on its neurobiology and the clinical role imaging will play. *Radiology* 2012;263:344-361
10. Kandel BM, Avants BB, Gee JC, McMillan CT, Erus G, Doshi J, et al. White matter hyperintensities are more highly associated with preclinical Alzheimer's disease than imaging and cognitive markers of neurodegeneration. *Alzheimers Dement (Amst)* 2016;4:18-27
11. Rauchmann BS, Ghaseminejad F, Mekala S, Perneczky R; Alzheimerr's Disease Neuroimaging Initiative. Cerebral microhemorrhage at MRI in mild cognitive impairment and early alzheimer disease: association with tau and amyloid β at PET imaging. *Radiology* 2020;296:134-142

12. Choy G, Khalilzadeh O, Michalski M, Do S, Samir AE, Pianykh OS, et al. Current applications and future impact of machine learning in radiology. *Radiology* 2018;288:318-328

13. Jung YH, Lee H, Kim HJ, Na DL, Han HJ, Jang H, et al. Prediction of amyloid β PET positivity using machine learning in patients with suspected cerebral amyloid angiopathy markers. *Sci Rep* 2020;10:18806

14. Kang SH, Cheon BK, Kim JS, Jang H, Kim HJ, Park KW, et al. Machine learning for the prediction of amyloid positivity in amnestic mild cognitive impairment. *J Alzheimers Dis* 2021;80:143-157

15. McKhann GM, Knopman DS, Chertkow H, Hyman BT, Jack CR Jr, Kawas CH, et al. The diagnosis of dementia due to Alzheimer's disease: recommendations from the National Institute on Aging-Alzheimer's Association workgroups on diagnostic guidelines for Alzheimer's disease. *Alzheimers Dement* 2011;7:263-269

16. Sabri O, Seibyl J, Rowe C, Barthel H. Beta-amyloid imaging with florbetaben. *Clin Transl Imaging* 2015; 3:13-26

17. Gordon BA, Najmi S, Hsu P, Roe CM, Morris JC, Benzinger TL. The effects of white matter hyperintensities and amyloid deposition on Alzheimer dementia. *Neuroimage Clin* 2015;8:246-252

18. Graff-Radford J, Lesnick T, Rabinstein AA, Gunter J, Aakre J, Przybelski SA, et al. Cerebral microbleed incidence, relationship to amyloid burden: the Mayo clinic study of aging. *Neurology* 2020;94:e190-e199

19. Linn J, Halpin A, Demaerel P, Ruhland J, Giese AD, Dichgans M, et al. Prevalence of superficial siderosis in patients with cerebral amyloid angiopathy. *Neurology* 2010;74:1346-1350

20. Yamada M. Cerebral amyloid angiopathy: emerging concepts. *J Stroke* 2015;17:17-30

21. Suh CH, Shim WH, Kim SJ, Roh JH, Lee JH, Kim MJ, et al. Development and validation of a deep learning–based automatic brain segmentation and classification algorithm for Alzheimer disease using 3D T1-weighted volumetric images. *AJNR Am J Neuroradiol* 2020;41:2227-2234

22. Jiang J, Liu T, Zhu W, Koncz R, Liu H, Lee T, et al. UBO detector - A cluster-based, fully automated pipeline for extracting white matter hyperintensities. *Neuroimage* 2018;174:539-549

23. Pedregosa F, Varoquaux G, Gramfort A, Michel V, Thirion B, Grisel O, et al. Scikit-learn: machine learning in python. *J Mach Learn Res* 2011;12:2825-2830

24. Abraham A, Pedregosa F, Eickenberg M, Gervais P, Mueller A, Kossaifi J, et al. Machine learning for neuroimaging with scikit-learn. *Front Neuroinform* 2014;8:14

25. Chu C, Hsu AL, Chou KH, Bandettini P, Lin C; Alzheimer's Disease Neuroimaging Initiative. Does feature selection improve classification accuracy? Impact of sample size and feature selection on classification using anatomical magnetic resonance images. *Neuroimage* 2012;60:59-70

26. Nguyen DT, Ryu S, Qureshi MNI, Choi M, Lee KH, Lee B. Hybrid multivariate pattern analysis combined with extreme learning machine for Alzheimer's dementia diagnosis using multi-measure rs-fMRI spatial patterns. *PLoS One* 2019;14:e0212582

27. Kang KM, Sohn CH, Byun MS, Lee JH, Yi D, Lee Y, et al. Prediction of amyloid positivity in mild cognitive impairment using fully automated brain segmentation software. *Neuropsychiatr Dis Treat* 2020;16:1745-1754

28. Kim JP, Kim J, Jang H, Kim J, Kang SH, Kim JS, et al. Predicting amyloid positivity in patients with mild cognitive impairment using a radiomics approach. *Sci Rep* 2021;11:6954

29. Koivunen J, Scheinin N, Virta JR, Aalto S, Vahlberg T, Någren K, et al. Amyloid PET imaging in patients with mild cognitive impairment: a 2-year follow-up study. *Neurology* 2011;76:1085-1090

30. Nestor SM, Rupsingh R, Borrie M, Smith M, Accomazzi V, Wells JL, et al. Ventricular enlargement as a possible measure of Alzheimer's disease progression validated using the Alzheimer's disease neuroimaging initiative database. *Brain* 2008;131(Pt 9):2443-2454

31. Moscoso A, Rey-Bretal D, Silva-Rodríguez J, Aldrey JM, Cortés J, Pías-Peleteiro J, et al. White matter hyperintensities are associated with subthreshold amyloid accumulation. *Neuroimage* 2020;218:116944

32. Kuroda T, Honma M, Mori Y, Futamura A, Sugimoto A, Yano S, et al. Increased presence of cerebral microbleeds correlates with ventricular enlargement and increased white matter hyperintensities in Alzheimer's disease. *Front Aging Neurosci* 2020;12:13

33. Thong JY, Hilal S, Wang Y, Soon HW, Dong Y, Collinson SL, et al. Association of silent lacunar infarct with brain atrophy and cognitive impairment. *J Neurol Neurosurg Psychiatry* 2013;84:1219-1225

34. Chen CF, Lan SH, Khor GT, Lai CL, Tai CT. Cognitive dysfunction after acute lacunar infarct. *Kaohsiung J Med Sci* 2005;21:267-271

뇌 MRI와 인지기능평가를 이용한 아밀로이드 베타 양성 예측 연구

박혜진[1] · 이지영[2]* · 양진주[3] · 김희진[4] · 김영서[4] · 김지영[5] · 최윤영[6]

목적 경도인지장애와 알츠하이머 치매 환자에서 아밀로이드베타 양성을 예측할 수 있는 MRI 특징을 알아보고 머신러닝으로 아밀로이드베타 양성 예측 모형의 성능을 알아보고자 하였다.

대상과 방법 후향적 및 단면조사연구로 경도인지장애와 알츠하이머 치매 총 139명의 환자를 대상으로 하였다. 이들은 모두 뇌 MRI와 아밀로이드 PET-CT를 시행하였다. 대상자는 아밀로이드 베타 양성군(n = 84)과 아밀로이드 베타 음성군(n = 55)으로 분류하였다. 시각적 분석으로는 뇌백질 고신호 병변의 Fazekas 척도와 뇌미세출혈 개수를 시행하였다. 정량분석으로 뇌백질 고신호 병변의 부피와 국소뇌부피를 측정하였다. 다중 로지스틱 회귀분석과 머신러닝 기법으로 아밀로이드베타 양성을 가장 잘 예측할 수 있는 MRI 특징을 확인하였다.

결과 시각적분석에서 아밀로이드베타 양성군은 뇌백질 고신호 병변의 Fazekas 척도(p = 0.02)와 뇌미세출혈 개수(p = 0.04)가 유의미하게 높았다. 해마, 내후각피질, 설전부의 국소뇌부피들은 아밀로이드베타 양성군에서 유의미하게 작았다(p < 0.05). 제3뇌실(p = 0.002)의 부피는 아밀로이드베타 양성군에서 유의미하게 컸다. 간이 정신 상태 검사와 국소뇌부피를 이용하여 머신러닝기법을 이용했을 때 좋은 정확도를 보였다(81.1%).

결론 간이 정신 상태 검사, 제3뇌실과 해마 부피를 이용한 머신러닝의 적용은 아밀로이드베타 양성을 예측하는데 활용될 수 있다.

한양대학교 의과대학 한양대학교병원 [1]영상의학과, [4]신경과, [6]핵의학과,
[2]가톨릭대학교 의과대학 서울성모병원 영상의학과,
[3]한양대학교 공과대학 바이오메디컬공학과,
[5]한양대학교 의과대학 구리한양대학교병원 핵의학과